

**Improved Axial Damping of Mechanical Elements  
Through the Use of Multiple Layered, Stress Coupled, Co-cured  
Damped Fiber Reinforced Composites**

**Angela Trego, Dennis D. Olcott, Paul F. Eastman**

Department of Mechanical Engineering  
Brigham Young University  
Provo, UT 84602

**ABSTRACT**

*Light weight, dynamically stiff composite structures with high levels of in-plane damping as well as the more common out-of-plane damping have been demonstrated. A computer model has been developed which predicts axial modulus and loss factor for single and multiple viscoelastic layers in the structures. The structures are created using layers of viscoelastic material sandwiched between orthotropic composite layers. The composite layers have different orientation angles, purposefully unsymmetric. Stress coupling between the stiffness layers when excited by in-plane or out-of-plane vibrations produces hysteresis losses that are distributed throughout the viscoelastic layers, resulting in vibrational damping.*

**1.0 INTRODUCTION**

Vibrations caused by engine noise, rotating parts, and air turbulence affect equipment in all industries including transportation, manufacturing, etc.. Controlling vibrations is often critical for sensitive components. Uncontrolled vibrations cause fatigue damage, structural failure at lower stresses, and noise in sensitive electronic equipment. Reducing vibrations can be accomplished by increasing the stiffness of the structural component or by reducing the source of the vibrations. Unfortunately, stiffening structures adds weight and can shift the damaging resonant frequencies to other structural components; reducing vibrations at the source is usually not a viable alternative.

There are two possible damping methods for controlling vibrations: passive damping and active damping. Passive damping can be accomplished relatively inexpensively. It uses part geometry and material changes to reduce vibrations. This is done inherently by converting kinetic energy (movement) to thermal energy. Examples of passive damping methods range from gas shock absorbers to padding on aluminum baseball bats. Active damping is usually more expensive. It requires a power source, a feedback control system, sensors and actuators (which are often combined).

Passive damping is limited primarily to out-of-plane displacement applications and is therefore limited in application and efficiency. The need for a power source, force transducers, sensors, and feedback control have made active damping methods difficult and expensive to implement, also resulting in limited application and efficiency. Many vibration problems have not been cost-effectively addressed using the current realm of passive and active damping technologies.

Fiber reinforced resins (composites) have an advantage over conventional materials in many applications because of their favorable strength to weight ratios, stiffness to weight ratios, corrosion resistance, and unique stress coupling properties. Composites have 10 to 100 times the damping of metals, but the damping is still low, less than 1% usually. Viscoelastic materials on the other hand, exhibit poor strength to weight ratios, but can provide impressive levels of damping when shear displacements are generated in the material. By combining the advantages of both composites and viscoelastics, it is possible to create a structure which is lightweight, stiff, and highly damped.

This paper outlines a new passive damping technology that is applicable to both in-plane displacements, as well as the traditional out-of-plane displacements.

## 2.0 BACKGROUND

One of the more common passive damping technologies is called Constrained Layer Damping (CLD) [Kerwin, 1959]. CLD is achieved by bonding a thin metal sheet, usually aluminum, to an existing structure with a viscoelastic adhesive. Deformations in the existing structure during vibration create shear displacements in the viscoelastic as the outer metal sheet tries not to move. Internal friction in the form of hysteresis losses in the viscoelastic material generates thermal energy, thus reducing the vibrational energy through heat dissipation. There are three major limitations of CLD:

- it adds weight and bulk
- it may only be applied to the surface of the structure
- it is only effective for out-of-plane vibrations

Barrett used the inherent shear coupling properties of composite materials to design a damped composite tubular component [Barrett, 1989] (see Figure 1).

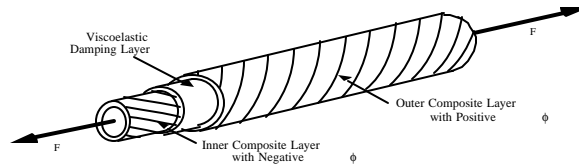


**Figure 1. Combination of constrained layer damping and shear coupling.**

Shear displacements occur naturally when fiber-reinforced composites are loaded in tension or compression along any axis not parallel or perpendicular to the fibers. The axial tension loads cause the fibers to straighten out, thus causing the shear displacements (see Figure 2). Constructing a plate with a layer of positive fiber angle orientation, a viscoelastic material layer, and a layer of negative fiber orientation will generate large shear strains when an axial load is applied, but only at the ends of the plate. These strains are caused by shear coupling, which comes from the coupling of shear strains and normal loads. Axial loads applied to tubular elements will cause the off-axis angles of a composite layer to rotate (see Figure 1). Barrett consequently designed a tube and combined the concepts of constrained layer damping with shear coupling to create the theoretical basis for a stiff, highly damped tube [Barrett, 1989]. The tubes which Barrett discussed contain a positive fiber orientation composite stiffness layer, a viscoelastic damping layer and a negative fiber orientation composite stiffness layer (see Figure 1). The tube would maintain high stiffness because the axial loads traveled through the composite material and high damping because shear strains were produced across the viscoelastic layer.

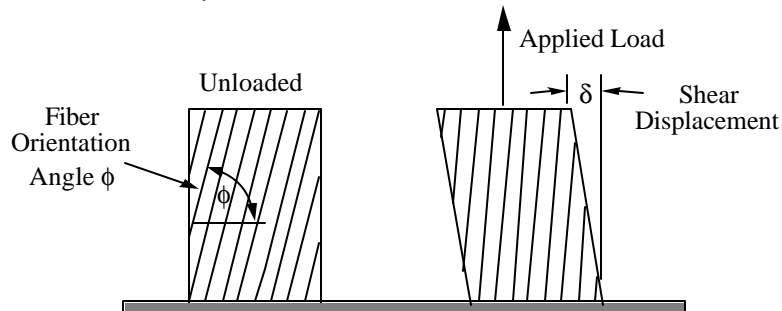


**Figure 2. Shear Displacements of fiber-reinforced composites.**

Unfortunately, Barrett's shear coupled tubes experienced shearing only at the ends of the tubes. Clamping the tube at the ends eliminated the damping effect, effectively reducing this tube to a conventional composite tube. Attaching to only the inner or outer tube reduced stiffness and damping which is also unacceptable.

A second design was proposed by Dolgin [Dolgin, 1991] concurrently with the method developed by Olcott. Dolgin suggested the construction of similar tubes using a chevron pattern for the fiber orientation. Similar to Barrett's design, the magnitude of damping in the tube is contingent on free movement of the ends.

Concurrently, Olcott developed a new damping concept called Stress Coupling Activated Damping (SCAD<sup>®</sup>) at Brigham Young University [Olcott, 1992]. SCAD<sup>®</sup> uses the stress coupling effect of anisotropic materials, such as fiber reinforced composites, to distribute damping through the entire volume of embedded viscoelastic layers. The key to SCAD<sup>®</sup> is that the fiber orientation angle is altered many times down the length of the structure. At each of the angle changes, a region of high shear stress is generated across the adjacent damping layer(s) (see figure 3). By controlling the orientation angle, thickness, segment lengths and moduli, significant shearing will now occur over most of the structure. Also, since the primary load path through the part remains in the composite layers, the part retains high stiffness. Even clamping the ends of the structure will only eliminate shearing at the ends, thus resulting in insignificant reductions of the overall damping effect [Olcott et al., 1992]. Most importantly, SCAD<sup>®</sup> provides damping for both in-plane as well as out-of-plane loads which makes it applicable to a wide range of structures and geometries, not just tubular structures.

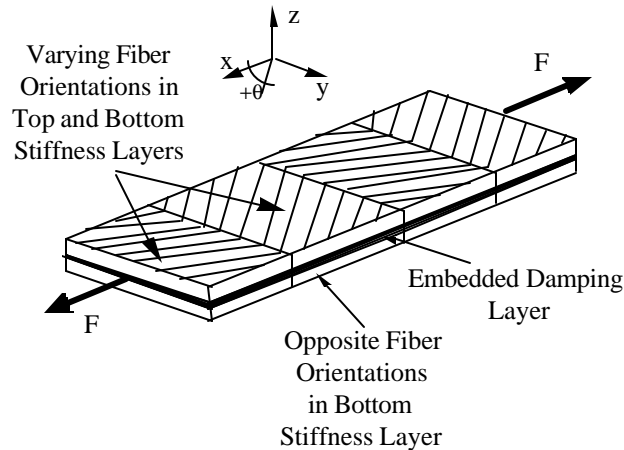


**Figure 3. Olcott's Damping Concept.**

[Barret, 1992], [He and Rao, 1992], [Sankar and Deshpande, 1993], [Saravanos, 1995], [Saravanos, 1992], [Sun, et al. 1990], and [Yi, et al., 1995] have analyzed natural frequencies and loss factors of passively damped composite structures. Their research has only been developed for the Constrained Layer Damping (CLD) theory. While the CLD theory provides significant improvements in damping for some structures, SCAD<sup>®</sup> technology, as shown below, will provide even greater damping for in-plane loading applications.

### 3.0 ANALYTIC MODELING

A single layer analytical model, first developed by Olcott [Olcott, 1992] is expanded in this paper to analyze multiple damping layer, passively damped composite structures. This model determines the loss factor, stiffness, stresses resulting from in-plane loading and axial natural frequencies of structures made with the SCAD<sup>®</sup> theory. While the CLD method only provides out-of-plane predictions, this model addresses the predictions of in-plane properties. Like CLD, SCAD<sup>®</sup> is constructed using an alternating system of stiffness and damping layers. The SCAD<sup>®</sup> structure will behave similar to a CLD structure for out-of-plane deformations. CLD structures may be analyzed using existing CLD methods. Current research is being conducted on out-of-plane applications with the SCAD<sup>®</sup> theory.

### 3.1 SCAD<sup>®</sup> Analytic Model

The SCAD<sup>®</sup> model, which determines the loss factor and the axial modulus of the overall structures, requires several assumptions [Olcott, 1992], summarized as follows:

- The stiffness layers are assumed to be thin with no out-of-plane shear deformation.
- The membrane may only be loaded axially,  $\sigma_{xx}$ , and in transverse shear,  $\tau_{xy}$ .
- Displacements are not a function of  $y$ , therefore  $du/dy = dv/dy = 0$  (see figure 3).
- The damping layer moduli are much lower than the stiffness layer moduli; hence all normal loads applied to the stiffness layers from damping layer deformations are assumed negligible.
- The only out-of-plane stress applied to the stiffness layers by the damping layers are the shear stresses  $\tau_{xz}$  and  $\tau_{yz}$ , which act through the neutral axis of the structure.
- There is no slip at the interface between a stiffness layer and a damping layer.
- Displacements in the  $z$ -direction are negligible, therefore  $dw/dx = dw/dy = 0$ .

#### 3.1.2 Damping Layers

From the above assumptions, the shear stresses in the damping layer are:

$$\tau_{xz} = G_d \frac{\check{z}v}{\check{z}z}, \quad \tau_{yz} = G_d \frac{\check{z}v}{\check{z}z} \quad (1)$$

Where  $G_d$  is the complex shear modulus of the damping layer defined by the equation:

$$G_d = G' + \eta G'' \quad (2)$$

Where:  
 $G'$  = storage shear modulus  
 $G''$  = loss shear modulus  
 $\eta$  = loss factor at the temperature and frequency of interest

Note that the following analysis variables are all complex variables:  $E_{11}$ ,  $E_2$ ,  $G_{12}$  (composite materials);  $G_d$  (damping material);  $Q$ ,  $K$ , and  $D_0$  (structural variables) thus the damping of each component of the structure is included in the analysis.

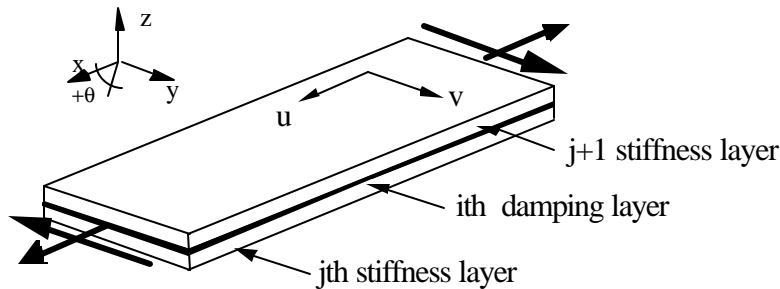


**Figure 4. Numbering scheme, coordinate convention and acceptable external loads.**

Stress equilibrium requires that the shear stresses be functions of  $x$  only. Equation 3 express the shear stresses in the damping layer entirely in terms of the displacements of the adjacent composite layers:

$$\tau_{xz} = G_d \left( \frac{u_{j+1} - u_j}{t_d} \right), \quad \tau_{yz} = G_d \left( \frac{v_{j+1} - v_j}{t_d} \right) \quad (3)$$

where  $u_j, u_{j+1}, v_j, v_{j+1}$  are the axial and transverse displacements of the lower and upper stiffness layers and  $t_d$  is the thickness of the damping layer under investigation (see figure 4).

### 3.1.3 Stiffness Layers

The general orthotropic stress-strain relationships applicable to composite stiffness layers represented in matrix notation are:

$$\begin{bmatrix} \sigma_{xx} \\ \sigma_{yy} \\ \tau_{xy} \end{bmatrix} = \begin{bmatrix} \bar{Q}_{11} & \bar{Q}_{12} & \bar{Q}_{16} \\ \bar{Q}_{21} & \bar{Q}_{22} & \bar{Q}_{26} \\ \bar{Q}_{61} & \bar{Q}_{62} & \bar{Q}_{66} \end{bmatrix} \begin{bmatrix} \epsilon_{xx} \\ \epsilon_{yy} \\ \gamma_{xy} \end{bmatrix} \quad (4)$$

The constants  $\bar{Q}_{11}$  through  $\bar{Q}_{66}$  are functions of the complex axial, transverse and shear moduli, poisson ratio, and the fiber orientation angle and may be found in any general composite material reference. From the analysis assumptions only  $\sigma_{xx}$  and  $\tau_{xy}$  stresses may be applied to the stiffness layers, implying that  $\sigma_{yy} = 0$ . The strain in the y-direction, however, is not zero due to poisson effects. Under these conditions equation 4 may be reduced to a 2x2 matrix (5) plus the equations for strain (9):

$$\begin{bmatrix} \sigma_{xx} \\ \tau_{xy} \end{bmatrix} = \begin{bmatrix} K_{11} & K_{16} \\ K_{61} & K_{66} \end{bmatrix} \begin{bmatrix} \epsilon_{xx} \\ \gamma_{xy} \end{bmatrix} \quad (5)$$

Where  $K_{11}$  through  $K_{66}$  are given by:

$$K_{11} = \bar{Q}_{11} - \frac{\bar{Q}_{12}\bar{Q}_{12}}{\bar{Q}_{22}} \quad (6)$$

$$K_{16} = K_{61} = \bar{Q}_{16} - \frac{\bar{Q}_{12}\bar{Q}_{26}}{\bar{Q}_{22}} \quad (7)$$

$$K_{66} = \bar{Q}_{66} - \frac{\bar{Q}_{26}\bar{Q}_{26}}{\bar{Q}_{22}} \quad (8)$$

The strains are given by:

$$\begin{bmatrix} \epsilon_{xx} \\ \gamma_{xy} \end{bmatrix} = \begin{bmatrix} \bar{Z}_u \\ \bar{Z}_x \\ \bar{Z}_v \\ \bar{Z}_x \end{bmatrix}, \quad \epsilon_{yy} = \frac{\bar{Q}_{12}\epsilon_{xx} + \bar{Q}_{26}\gamma_{xy}}{\bar{Q}_{22}} \quad (9)$$

The differential stiffness layer element shown in Figure 5 shows the stresses assumed to be acting upon the element,  $\sigma_{xx}$  and  $\tau_{xy}$ . The adjacent damping layers exert shear stresses  $\tau_{xzlower}$  and  $\tau_{yzlower}$  on the bottom surface and  $\tau_{xzupper}$  and  $\tau_{yzupper}$  on the top surface.

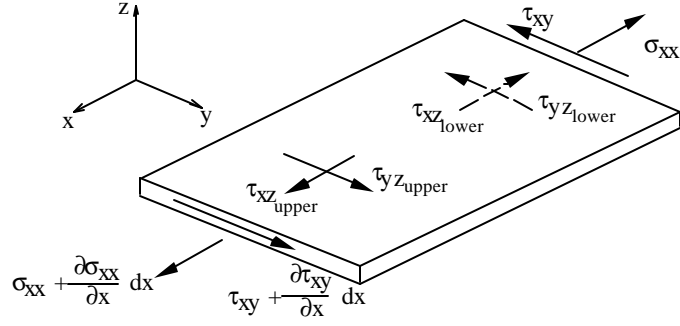


**Figure 5. Stress equilibrium diagram for a stiffness layer element  $dx$  by  $dy$ , and thickness  $t_s$ .**

Force equilibrium in the axial direction is maintained when:

$$\frac{\partial \sigma_{xx}}{\partial x} t_s + (\tau_{xz\_upper} - \tau_{xz\_lower}) = 0 \quad (10)$$

Equation 10 can be simplified to an equation involving displacements only using the normal strain-displacement relations from elasticity theory and the previous damping layer shear stress equations:

$$K_{11j} \frac{\partial^2 u}{\partial x^2} + K_{16j} \frac{\partial^2 v}{\partial x^2} + (G_j) \left[ \frac{(u_{j+1} - u_j)}{t_s t_d} \right] = 0 \quad (11)$$

where:  $j$  = stiffness layer  
 $j+1$  = stiffness layer above  
 $i$  = damping layer above the stiffness layer

By following the same procedure an equation for the y-direction force equilibrium may also be developed:

$$K_{16j} \frac{\partial^2 u}{\partial x^2} + K_{66j} \frac{\partial^2 v}{\partial x^2} + (G_j) \left[ \frac{(v_{j+1} - v_j)}{t_s t_d} \right] = 0 \quad (12)$$

These governing equations (11 and 12) for a single stiffness layer may be combined into a matrix form and non-dimensionalized by dividing by  $E_{11}$ , and a reference length  $L$  (usually the length of a segment):

$$\begin{bmatrix} \hat{K}_{11} & \hat{K}_{16} & 0 & 0 \\ \hat{K}_{16} & \hat{K}_{66} & 0 & 0 \\ 0 & 0 & \hat{K}_{11} & -\hat{K}_{16} \\ 0 & 0 & -\hat{K}_{16} & \hat{K}_{66} \end{bmatrix} \begin{bmatrix} \frac{\partial^2 \hat{u}}{\partial \hat{x}^2} \\ \frac{\partial^2 \hat{v}}{\partial \hat{x}^2} \\ \frac{\partial^2 \hat{u}}{\partial \hat{x}^2} \\ \frac{\partial^2 \hat{v}}{\partial \hat{x}^2} \end{bmatrix} + \hat{D}_0 \begin{bmatrix} 1 & 0 & -2 & 0 \\ 0 & 1 & 0 & -2 \end{bmatrix} \begin{bmatrix} \hat{u}_1 \\ \hat{v}_1 \\ \hat{u}_2 \\ \hat{v}_2 \end{bmatrix} = 0 \quad (13)$$

where:

$$\begin{aligned}
\hat{K}_{pq} &= \frac{K_{pq}}{E_{11}} && \text{a function of the complex modulus } E_{11}, \phi \text{ and } \nu \text{ for the stiffness layer} \\
\hat{u} &= \frac{u}{L_s} && \text{displacements in the axial direction divided by the segment length} \\
\hat{v} &= \frac{v}{L_s} && \text{displacements in the transverse direction divided by the segment length} \\
\frac{\check{Z}^2 u}{\check{Z}_X^2} &= \left( \frac{1}{L_s} \right) \frac{\check{Z}^2 \hat{u}}{\check{Z}_X^2} && \text{by applying the partial derivative chain rule} \\
\frac{\check{Z}^2 v}{\check{Z}_X^2} &= \left( \frac{1}{L_s} \right) \frac{\check{Z}^2 \hat{v}}{\check{Z}_X^2} && \text{by applying the partial derivative chain rule} \\
D_o &= \frac{G_d L_s^2}{E_{11} t_s t_d} && \text{a function of the damping layer and adjacent stiffness layer}
\end{aligned}$$

Trego expanded this theory into a more general model including the possibility of having several damping and stiffness layers and applying different types of viscoelastic material either symmetrically or non-symmetrically to the structure, as well as having an unlimited number of segments. Multiple damping layers gives a higher potential for energy absorption, thus more damping may be attained while still maintaining a stiffness design limit. In this manner, a designer may also better tune a structure in order to optimize the damping and stiffness in multiple frequency ranges.

A more general non-dimensionalized number is defined for multiple damping layers which allows for different damping materials and different thickness of both the damping and stiffness layers to be incorporated into the design. The new non-dimensionalized number is:

$$D_{O_{ji}} = \frac{G_{d_i} L_s^2}{E_{11j} t_{s_j} t_{d_i}} \quad (14)$$

where:  $i = j$  for the damping layer above the stiffness layer  
 $j = j-1$  for the damping layer below the stiffness layer

Two of these modified non-dimensionalized numbers are calculated for each stiffness layer corresponding to the damping layer below ( $D_{O_{j,j-1}}$ ) and above ( $D_{O_{j,j}}$ ) the stiffness layer ( $j$ ). By recalculating the modified non-dimensionalized number in each layer, different materials, thicknesses and lengths are allowed in the design. These variations will be especially advantageous for structures subjected to vibrations in several frequency ranges and temperatures.

For multiple viscoelastic layers, equilibrium must still be satisfied. The general equations for each stiffness layer are similar to the single layer model:

$$\begin{bmatrix} \hat{K}_{11j} & \hat{K}_{16j} \\ \hat{K}_{16j} & \hat{K}_{66j} \end{bmatrix} \begin{bmatrix} \frac{\check{I}^2 \hat{u}_j}{\check{I}^2 X} \\ \frac{\check{I}^2 \hat{v}_j}{\check{I}^2 X} \end{bmatrix} + \begin{bmatrix} D_{O_{(j,j-1)}} & 0 & -D_{O_{(j,j)}} - D_{O_{(j,j-1)}} & 0 & D_{O_{(j,j)}} & 0 \\ 0 & D_{O_{(j,j-1)}} & 0 & -D_{O_{(j,j)}} - D_{O_{(j,j-1)}} & 0 & D_{O_{(j,j)}} \end{bmatrix} \begin{bmatrix} \hat{u}_{(j-1)} \\ \hat{v}_{(j-1)} \\ \hat{u}_j \\ \hat{v}_j \\ \hat{u}_{(j+1)} \\ \hat{v}_{(j+1)} \end{bmatrix} = 0 \quad (15)$$

The equilibrium equations for all stiffness layers may again be combined into a square matrix. The combined matrix will be a  $[2n \times 2n]$  dimension square matrix for  $n$  number of stiffness layers. Note that the bottom layer ( $j=1$ ) and the top layer ( $j = n$ ) will have zero terms in the combined matrix when referring to non-existent damping layers.

The corresponding combined matrix will be of the general form:

$$[\hat{\mathbf{K}}_j] \frac{\ddot{\mathbf{Z}}}{\ddot{\mathbf{X}}} [\hat{\mathbf{U}}_j] + [\mathbf{D}_{oi}] [\hat{\mathbf{U}}_j] = 0 \quad (16)$$

The eigenvalues and eigenvectors,  $\lambda_j$  and  $[\hat{\mathbf{U}}_{0j}]$ , are found by solving the linear eigensystem:

$$(\lambda^2 [\hat{\mathbf{K}}_j] + [\mathbf{D}_{oi}]) [\hat{\mathbf{U}}_j] = 0 \quad (17)$$

An eigensystem of this form must be solved for each segment in the structure. The displacement solution to the eigenvalue equation is of the form:

$$\begin{bmatrix} \hat{u}_1 \\ \hat{v}_1 \\ \cdots \\ \cdots \\ \hat{u}_n \\ \hat{v}_n \end{bmatrix} = \sum_{j=1}^n \begin{bmatrix} \hat{u}_1 \\ \hat{v}_1 \\ \cdots \\ \cdots \\ \hat{u}_n \\ \hat{v}_n \end{bmatrix}_0 \left[ \hat{c}_{+j} e^{(\lambda)_x} + \hat{c}_{-j} e^{(-\lambda)_x} \right] \quad (18)$$

The constants  $\hat{c}_{+j}$  and  $\hat{c}_{-j}$  are found by applying the appropriate load and displacement boundary conditions on the segment being modeled in equation 18. Particular analysis elements may be found which allow a small section of the whole component to be efficiently modeled, which will then yield the solution to the entire original component.

From this solution an effective axial modulus of elasticity is calculated along with the first mode axial frequency and loss factor of the structure according to:

$$E_{axial} = \frac{\sum_{i=1}^n \sigma_{axial}}{\epsilon_{axial}} \quad (19)$$

$$f = \frac{1}{2L_p} \sqrt{\frac{E_{axial}}{\rho}} \quad (20)$$

$$\eta = \frac{E''_{axial}}{E'_{axial}} \quad (21)$$

Where:  $E_{axial}$  = axial modulus  
 $E'$  = real component of the axial modulus  
 $E''$  = complex component of the axial modulus  
 $L_p$  = total length of the part  
 $\rho$  = average density of the structure

The axial strain is the total axial deflection of the structure divided by the total length (also the average of all axial strains which will vary along the length). The axial stress is the total axial load on the structure divided by the total

cross-sectional area (also the average axial stress which will vary between layers, but will be constant at any given cross section). Similarly an effective shear modulus and loss factor may be calculated. Pay particular attention to the fact that this solution is only valid for a particular vibration frequency and temperature because  $G_d$ , the damping material complex modulus, is strongly dependent upon frequency and temperature. The computed moduli do not vary much with  $G_d$ , but the loss factor will change significantly, both because of the change in loss factor of the damping material and because of the change in  $D_0$  number.

#### 4.0 EXPERIMENTATION

Several passively damped composite tubes were made to test the analytic model. The composite tubes were tested in axial vibration at Brigham Young University using Andriulli's composite tube test method [Andriulli, 1989]. The tubes were suspended at each end by soft rubber bands to approximate free-free boundary conditions. Axial motion of the tube was monitored by attaching the accelerometer to one end, then striking the opposite end with a force hammer (see Figure 6). The force and acceleration signals were fed into the structural analyzer, which calculated the transfer function. The tube was struck 32 times to obtain good coherence, and the data averaged by the HP5423A analyzer. Damping values were calculated using the half-power method.

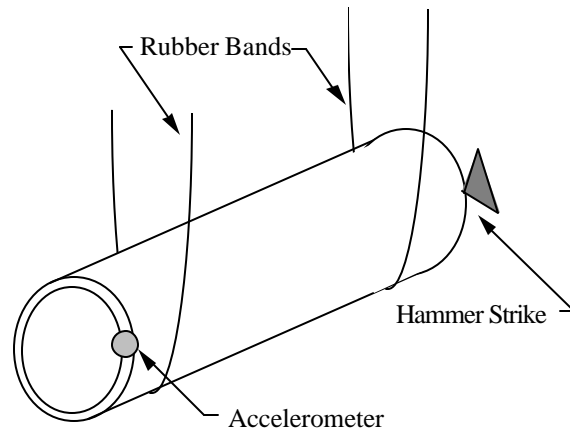


**Figure 6. Data acquisition setup.**

Table 1 shows the predicted versus the measured results for both the resonant frequency and the loss factors of a conventional composite tube and two of the several designs for damped composite tubes. These tubes were chosen to show an example of the variation of design parameters as well as a comparison to the CLD method.  $t_d$  is the thickness of the viscoelastic material or damping layer.  $\theta$  is the angle of the fiber orientation,  $L_s$  is the segment length and  $L_p$  is the part length.

Two conclusions may be made from Table 1. First, the two tube designs using the SCAD<sup>®</sup> technology improved the damping over the benchmark, or CLD composite tube design. While stiffness decreased by only 16% the damping increased by over 350%. Secondly, the program can predict within 5% for resonant frequencies and 20% for loss factors. The predictions for the damped tubes may not be as accurate because manufacturing methods for the damped tubes are not as well developed as they are for conventional tubes. Thus, manufacturing errors affected all of the measurements, and had a significant effect on the loss factor measurements. Also, the material properties used for design calculations have up to 10% error due to measurement methods.

**Table 1. Measured and predicted frequencies and loss factors for tubes.**

| Tube Specimens<br>(Damping Material/ $t_d$ / $\theta$ / $L_s$ / $L_p$ ) | Measured |      | Predicted |      |
|-------------------------------------------------------------------------|----------|------|-----------|------|
|                                                                         | (kHz)    | (%)  | (kHz)     | (%)  |
| ISD112/0.01"/26°/N.A./20.04"                                            | 4.75     | 2.36 | 4.56      | 2.02 |
| ISD112/0.01"/26°/3.0"/20.93"                                            | 4.10     | 8.50 | 4.02      | 10.7 |
| ISD112/0.005"/16°/2.5"/21.80"                                           | 6.41     | 2.77 | 6.58      | 2.73 |

Table 2 shows the predicted versus the measured results for both the resonant frequency and the loss factors of two of the several designs for damped composite tubes with multiple stiffness layers.  $t_d$  is the damping layer thickness. The fibre angle orientation is  $25^\circ$  with a segment length of 3.0",  $L_p$  is the length of the part and n is the number of stiffness layers.

**Table 2. Measured and predicted frequencies and loss factors for tubes.**

| Tube Specimens<br>(Damping Material/ $t_d$ / $L_p$ /n) | Measured |      | Predicted |      |
|--------------------------------------------------------|----------|------|-----------|------|
|                                                        | (kHz)    | (%)  | (kHz)     | (%)  |
| ISD112 / 0.03" / 20.02" / 6                            | 4.85     | 3.10 | 4.99      | 3.09 |
| ISD112 / 0.03" / 20.93" / 4                            | 4.80     | 7.30 | 4.86      | 6.70 |

As can be seen from Table 2, the multiple layer prediction model is also proven correct. The axial first frequency was predicted to within 3% and the loss factor to within 10%. It is interesting to note that although the damping is lowered with more layers, stiffness increased with more layers.

## 5.0 CONCLUSIONS & RECOMMENDATIONS

SCAD<sup>®</sup> is a structure created using layers of viscoelastic material sandwiched between orthotropic composite layers. In this paper a general model has been presented which allows for the prediction of the axial modulus and loss factor of a SCAD<sup>®</sup> dampened structure. SCAD<sup>®</sup> technology can be applied to a wide range of designs, especially structures with in-plane deformations, unlike the CLD technology which is limited to out-of-plane loads. For example, I-beams which primarily have in-plane loading in the flanges will benefit from this theory. First the SCAD<sup>®</sup> theory was expanded to include multiple stiffness layers and then a computer model was generated. The model shows correlation within 5% for resonant frequencies and 20% in damping.

Research at Brigham Young University focuses on improving the performance, manufacturability, and extending the uses of SCAD<sup>®</sup> related technology and concepts. The following areas of future research have been identified:

- Develop out-of-plane loading application prediction models.
- Improve manufacturing methods for:
  - zig zag prepreg with specified angle orientation.
- Manufacturing and design of:
  - machine tool components, active control integration, aerospace structures, panels, marine structures, automotive components and structures, metrology components, and noise control.

## BIBLIOGRAPHY

- J. Andriulli, "Measured Damping and Modulus of Composite Cylinders," *Proceeding of Damping '89*, BCC-1-26 (1989).
- D. Barrett, "A Design for Improving the Structural Damping Properties of Axial Members," *Proceeding of Damping '89*, HCB-1-18 (1989).
- D. Barrett, "An Anisotropic Laminated Damped Plate Theory," *Journal Sound and Vibration*, Vol. 153, No. 3, pg.453-465, (1992).
- B. Dolgin, "Composite Struts Would Damp Vibrations," *NASA Technical Briefs*, **15**: 79 (1991).
- S. He and M. Rao, "Damping of Laminated Composite Beams with Multiple Viscoelastic Layers," *JProceedings of the 2nd International Congress on Recent Developments in Air and Structure Borne Sound and Vibration* Auburn University, Alabama, pg.265-270, (1992).
- E. Kerwin, "Damping of Flexural Waves by a Constrained Viscoelastic Layer," *Journal of the Acoustical Society of America*, **31** (7) 952 (1959).
- D. Mead and S. Markus, "The Forced Vibration of a Three-Layer, Damped Sandwich Beam with Arbitrary Boundary Conditions," *Journal Sound and Vibration*, Vol. 10, pg.163-175, (1969).
- D. Olcott, "Improved Damping in Composite Structures Through Stress Coupling, Co-Cured Damping Layers, and Segmented Stiffness Layers," Ph.D. Dissertation, Brigham Young University, Provo, Utah (1992).
- D. Olcott, C. Rotz, D. Barrett, "Cocured Damping Layers in Composite Structures," *Proceedings 23rd International SAMPE Technical Conference*, **23** 373 (1991).
- C. Rotz, and D. Barrett, "Co-cured Damping Layers in Composite Structures," *SAMPE Quarterly* **23** 2 42 (1992)
- B. Sankar and A. Deshpande, "Passive Damping of Large Space Structures," *AIAA Journal*, Vol. 31, No. 8, pg.1511-1516, (1993).

D. Saravanos and J. Pereira, "The Effects of Interply Damping Layers on the Dynamic Characteristics of Composite Plates," *AIAA Journal*, Vol. 30, No. 12, pg.2906-2913, (1992).

D. Saravanos and J. Pereira, "Dynamic Characteristics of Specialty Composite Structures with Embedded Damping Layers," *Transactions of the ASME*, Vol. 117, pg.62-68, (1995).

C. Sun, B. Sankar and V. Rao, "Damping and Vibration Control of Unidirectional Composite Laminates Using Add-On Viscoelastic Materials," *Journal Sound and Vibration*, Vol. 139, No. 2, pg.277-287, (1990).

S. Yi, M. Ahmad and H. Hilton, "Dynamic Responses of Plates with Viscoelastic Free Layer Damping Treatment," *Journal Vibration and Acoustics*, Vol. 117, pg.1-5, (1995).

## **BIOGRAPHIES**

Angela Trego is currently working on her Ph.D. at Brigham Young University with an emphasis in material science. Her research focuses on the development of passively damped composite structures. Ms. Trego is a member of Tau Beta Pi, Phi Kappa Phi, American Society of Mechanical Engineering, and Society of Women Engineers. She graduated from BYU with a M.S. in Mechanical Engineering and magna cum laude with her B.S. in Mechanical Engineering. For her master's degree, Ms. Trego developed a tolerance analysis program integrated into AutoCAD which is now being marketed. She recently received the NSF Graduate Fellowship Award.

Dennis D. Olcott received his Ph.D. and B.S. in Mechanical Engineering from Brigham Young University. He has worked for LTV Aircraft Products; AIM Aviation; Cirrus Design Corp.; and he currently works for Pacific Aviation Composites, USA. His professional interests include the appropriate application of advanced composite materials in general aviation aircraft, static and dynamic structural analysis, and advanced damping concepts.

Dr. Paul F. Eastman, Ph.D. is associate professor of mechanical engineering and associate director of the Advanced Composites Manufacturing and Engineering Center at Brigham Young University. He received his B.A. degree in physics and Ph.D. in ceramic engineering at the University of Utah. He worked for DuPont Company for 20 years in new product and process development for polymer film products before joining the Brigham Young University faculty. Professor Eastman's teaching and research interests are in the areas of materials and materials applications.